Supporting Information

Ms. ID: ac-2014-01004a

18 May, 2014

A simple, sensitive, and quantitative electrochemical detection method for paper analytical devices

Karen Scida,[1] Josephine Cunningham,[1] Christophe Renault,[1] Ian Richards,[2] Richard M. Crooks[1,*]

[1]Department of Chemistry, The University of Texas at Austin, 105 E. 24th Street, Stop A5300, Austin, Texas 78712-1224, USA

[2]Interactives Executive Excellence LLC, 201 N. Weston Lane, Austin, Texas 78733, USA

Table of Contents

S-1	Cover Page
S-2 – S-8	Experimental Section
S-9	Spontaneous Oxidation of AgNPs by $KMnO_4$
S-10 – S11	Effect of PBCl on the Electrochemical Signal
S-12	Background Fluorescence Micrographs for Figure 3
S-13	Evidence for the Formation of the Model Analyte
S-14	Optimization of the Electrochemical Signal
S-15 – S16	Insulation of the Electrode Surface by MnO_2
S-17 - S18	Optimization of $KMnO_4$ re-solvation time
S-19	References

19 Pages

Experimental Section

Instrumentation. An iPhone 5 was used to record Movie S1 and take the photographs shown in Figures S1a and S1b. Figures 3b, 3c, S5, and S8 were obtained using a Nikon AZ100 (Nikon Co., Tokyo, Japan) microscope equipped with a mercury lamp (Nikon) and a CCD camera (Cascade, Photometrics Ltd., Tucson, AZ) and using V^{++} Precision Digital Imaging software (Digital Optics, Auckland, New Zealand). All fluorescence images in Figure 3 and Figure S5 were taken using an HQ:F filter (λ_{ex} = 460-500 nm, λ_{ex} = 510-560 nm). All images were captured using 1 x 1 binning with 512 x 290 pixels and 1 s exposure time. The brightness and contrast of Figures 3b, 3c, and S5 were adjusted using ImageJ 1.45s software to enhance visualization of the fluorescence. The ASVs shown in Figures 1a and 4a were baseline corrected using Origin Pro8 SR4 v8.0951 (Northampton, MA).

Modification of citrate-capped AgNPs with biotinylated DNA. First, 10.0 μL of a 100.0 μM biotin-DNA-thiol solution and 600.0 μL of 0.75 nM citrate-capped AgNPs were mixed at 25 °C while vortexing (level 3) for 24 h. Second, the salt concentration in the solution was slowly increased to 70.0 mM NaCl and 7.0 mM phosphate buffer by adding one aliquot of 2.5 μL of 5.0 M NaCl and one aliquot of 25.0 μL of 50.0 mM phosphate buffer (pH 7.0) every day for 4 days. Third, the volume of the solution was slowly reduced to 250.0 μL using vacuum centrifugation at 40 °C for 3 h. Fourth, the resulting solution was centrifuged at 16,000 g for 20.0 min and the supernatant was removed. Fifth, the resulting biotinylated AgNPs were re-suspended in 600.0 μL of a solution containing 100.0 mM NaCl and 10.0 mM phosphate buffer (pH 7.0). This washing procedure (centrifugation, removal of supernatant, and resuspension) was repeated a total of three times.

The presence of the biotin/DNA/thiol on the surface of the AgNPs was confirmed by fluorescence as follows. The washed biotinylated AgNP solution was incubated with an aqueous solution of AlexaFluor-647/streptavidin conjugate (50.0 μg/mL final concentration) at 25 °C for 30 min while vortexing (level 3). The resulting AlexaFluor-647/streptavidin/biotin/AgNP solution was washed three times following the procedure described previously. At the same time, a control experiment was performed wherein 600.0 μL of 0.75 nM citrate-capped AgNPs (original concentration used in the synthesis of biotinylated AgNPs) was incubated with the AlexaFluor-647/streptavidin conjugate (50.0 μg/mL final concentration) at 25 °C for 30 min while vortexing (level 3). Next, aliquots from each experiment (test and control) were placed in a microtiter plate and their fluorescence was read using a microplate reader (λ_{ex} = 652 nm, λ_{em} = 688 nm). The fluorescence recorded for the test experiment was 87% higher than that of the control experiment, (data not shown), confirming biotinylation of the AgNPs.

Preparation of the AgNP/biotin/streptavidin/magnetic microbead model analyte. First, 100.0 μL of a stock solution of streptavidin-coated magnetic microbeads (1.11 pM, 2.8 μm in diameter) was placed in a microcentrifuge tube and a magnet was held against the tube (on a side wall) for 30 s, followed by the removal of the supernatant. Second, the microbeads were washed three times with 50.0 μL of 10.0 mM phosphate buffer (pH 7.4) by placing the magnet against one of the tube's wall for 30 s and removing the supernatant between washes. Third, after the third wash the magnetic microbeads were re-suspended in 200.0 μL of the previously synthesized biotinylated AgNPs solution. Fourth, the AgNPs and magnetic microbeads were incubated at 25 °C for 30 min while vortexing (level 3) and then washed three times with 100.0 μL of 10.0 mM phosphate buffer (pH 7.4) containing 100.0 mM NaCl.

Figure S6 shows the UV-Vis spectra of the supernatant (after removing the magnetic microbeads via magnetic separation), before (red trace) and after (blue trace) incubation with streptavidin-coated magnetic microbeads. The peaks at 400 and 510 nm on the red trace are attributed to the plasmon excitation of individual and agglomerated AgNPs, respectively. The band at 260 nm corresponds to the absorption of the DNA coating the AgNPs. The large absorbance decrease at 400 and 510 nm indicates the successful attachment of the AgNPs to the magnetic microbeads.

After synthesizing the AgNP/biotin/streptavidin/magnetic microbeads model analyte, the AgNP concentration in the model analyte solution was calculated by adding 125.0 μL of PBCl, 50.0 μL of 187.0 μM $KMnO_4$, 3.0 μL of model analyte, and 47.0 μL of deionized water to the PTFE cell configured in the *Facing Up* conventional electrochemical setup (Figure S1a). After performing the electrodeposition and stripping steps as described in the main text, the average charge measured (three repetitions) was correlated to the concentration of AgNPs in the stock model analyte solution (533 pM or 961 AgNP/magnetic microbead) using the calibration curve shown in Figure 1b.

Modification of streptavidin-coated magnetic microbeads with a biotin/fluorescein conjugate. First, 18.0 μL of stock streptavidin-coated magnetic microbeads were placed in a microcentrifuge tube and washed three times with 100.0 μL of 10.0 mM phosphate buffer by placing a magnet close to one of the tube's side wall for 30 s. Second, after the third wash, the microbeads were re-suspended in an aqueous solution containing 100.0 μL of 62.0 μM biotin/fluorescein conjugate and incubated at 25 °C with vortexing (level 3) for 30 min. Third, the resulting fluorescein/magnetic microbead conjugate were washed three times with 100.0 μL of 10.0 mM phosphate buffer. Fourth, after the last

wash, the beads were re-suspended in 100.0 μL of 10.0 mM phosphate buffer and stored at 4 °C in the dark until used.

Background run for ASVs obtained using the conventional electrochemical setup. A background ASV in the presence of 125.0 μL of PBCl, 50.0 μL of 187.0 μM $KMnO_4$, and 50.0 μL of deionized water was always performed between measurements to assure the surface of the glassy carbon electrode (GCE) was clean. After each background experiment and before each test run, the GCE was polished with microcut paper for 1 min, rinsed with deionized water, and dried with Kimwipes (these last three steps were repeated when necessary until the GCE was free of Ag).

Preparation of carbon ink for stencil printing. Prior to printing the carbon electrodes on the paper device, the carbon paste was thickened by adding a 0.5-cm thick layer of carbon paste to a glass vial and placing it in an oven at 65 °C for 30 min. Next, the vial was removed from the oven, the paste mixed with a glass rod, and the vial placed in the oven at 65 °C for 5 min. This re-heating step was performed a total of two times. The thickened paste was left to cool at 25 °C until needed.

Addition of electrical contacts to stencil-printed carbon electrodes. After the electrodes were stencil printed and dried, a piece of Parafilm paper was placed on top of the circular section of the electrodes (Figure S2) and copper epoxy was applied at the end of each electrode, followed immediately by placement of a strip of copper tape on top of the copper epoxy. The Parafilm was removed and the devices were placed in the oven at 60 °C for 1 h to cure the copper epoxy and enhance the electronic properties of the carbon paste. Once the devices were removed from the oven, a thin layer of insulating epoxy was placed over all the electrodes except in the circular areas. After the epoxy was completely dry (30 min at 25 °C), a thin layer of nail polish was applied over it to make the surface

more hydrophobic. The nail polish was also dried for 30 min at 25 °C.

Reagent loading on the *o*Slip. The blue dye and $KMnO_4$ were dispensed and dried onto their respective locations in the *o*Slip (see main text) by evaporation in air and under nitrogen flow (25 °C), respectively.

Drying conditions for measuring the capture efficiency of the model analyte at the WE of the *o*Slip. In the flow/capture test, after adding the final solution (2.0 μL of 10.0 mM phosphate buffer containing 0.2 pM fluorescein-labeled magnetic microbeads in 48.0 μL of PBCl) to the *Inlet* of the *o*Slip, the device was left to dry at 25 °C for 2 h in the dark. At this point, the device was opened and the fluorescence at the *WE* was measured (Figure 3b). In the control experiment, the solution dispensed on the *WE* (2.0 μL of 10.0 mM phosphate buffer containing 0.2 pM fluorescein-labeled magnetic microbeads) was left to dry at 25 °C for 2 h in the dark. Once the solution was dry, its fluorescence was measured (Figure 3c).

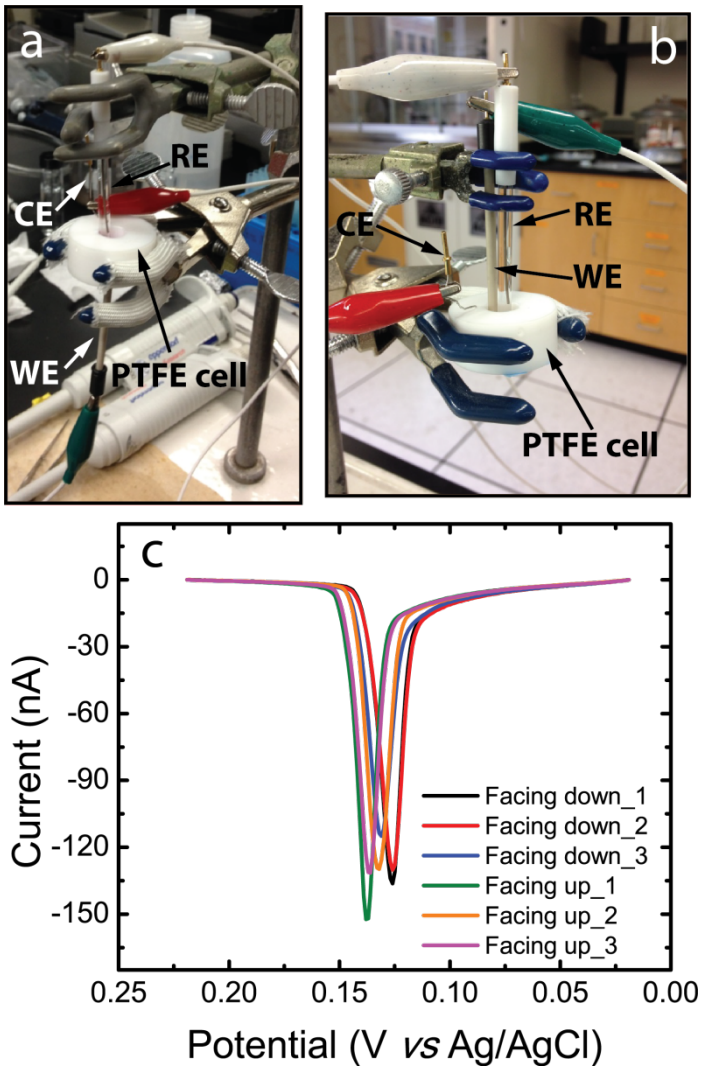

Figure S1. Conventional electrochemical cell used to study AgNP dissolution, electrodeposition, and anodic stripping voltammetry. (a) Photograph of the *Facing Up* electrode arrangement. In this case the GCE was placed tightly in its position using PTFE tape (to avoid leaking). (b) Photograph of the *Facing Down* electrode arrangement. (c) Anodic stripping voltammetry performed in triplicate using the *Facing Up* and *Facing Down* arrangements. υ: 10 mV/s; working electrode: glassy carbon, diameter = 1.0 mm; Ag/AgCl (1 M KCl) reference electrode; Pt wire counter electrode. See main text for details about the experiment.

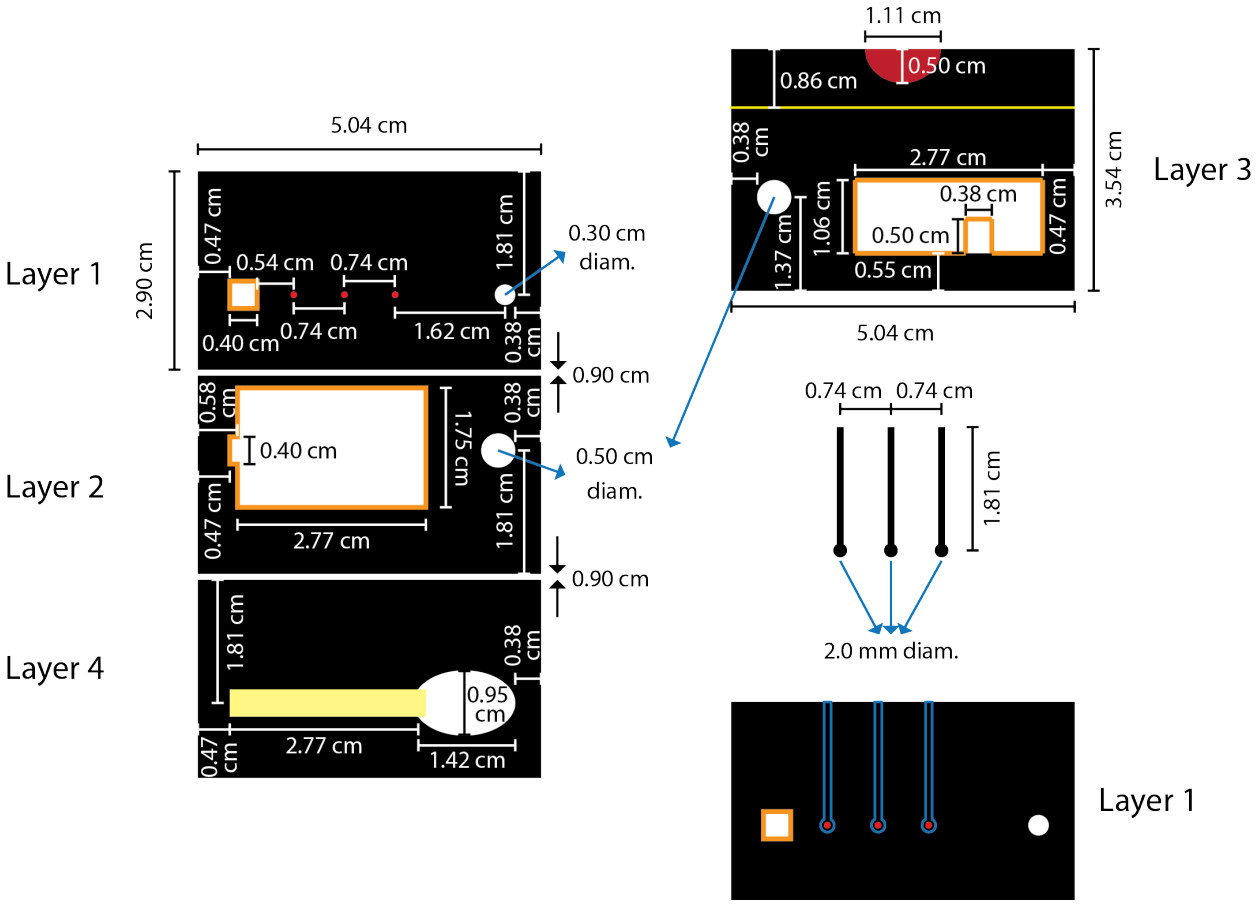

Figure S2. *o*Slip and stencil design and dimensions. *Left*: *o*PAD portion of the *o*Slip. *Top right*: SlipPAD portion of the *o*Slip. *Middle right*: Stencil electrode design. The black areas were cut using a laser engraving system. The width of the rectangular leads is 1.0 mm. *Bottom right*: Position of the stencil on Layer 1. The red dots on Layer 1 serve as a point of reference for alignment. The blue lines represent the outline of the cut stencil.

Spontaneous oxidation of AgNPs by $KMnO_4$

Two experiments were performed to confirm spontaneous oxidation of AgNPs in the presence of $KMnO_4$. In the first, 625.0 μL of PBCl and 250.0 μL of 75.0 pM citrate-capped AgNPs were placed in a microcentrifuge tube. Next, 250.0 μL of 187.0 μM $KMnO_4$ were added and, after 30 s, the tube was placed in the nanoparticle tracking instrument for analysis. In the second experiment (the control), 625.0 μL of PBCl, 250.0 μL of 75.0 pM citrate-capped AgNPs, and 250.0 μL of deionized water were placed in a microcentrifuge tube and analyzed. For each experiment, the solution was analyzed a total of three times. Citrate-capped AgNP diameters of 13 ± 3 and 21 ± 1 nm were obtained for the experiments in the presence and absence of $KMnO_4$, respectively (Figure S3).

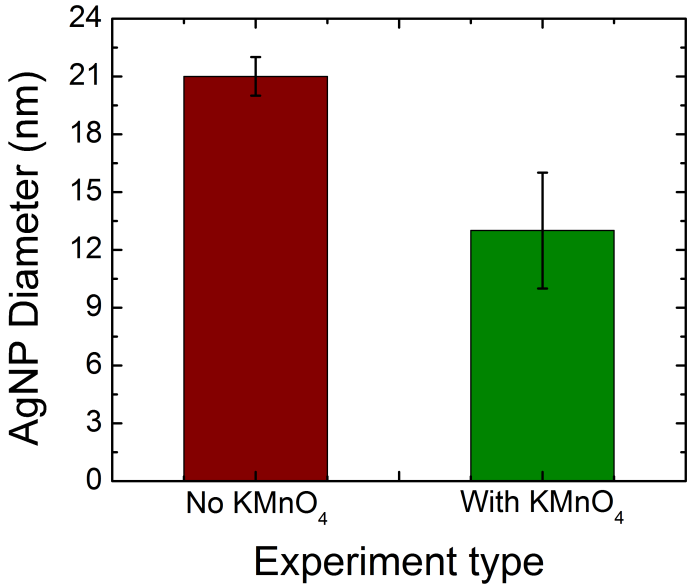

Figure S3. Histogram showing the size distribution of AgNPs in the presence and absence of 187.0 μM $KMnO_4$ as measured with the nanoparticle tracking instrument (Nanosight).

Effect of Cl^- and PO_4^{3-} on the electrochemical signal

The effect of Cl^- (present in the electrolyte) on the electrochemical signal was examined by performing two experiments. Both experiments were carried out using the conventional electrochemical setup in the *Facing up* configuration (Figure S1a). In the first experiment, 50.0 μL of 75.0 pM citrate-capped AgNP, 125.0 μL of PBCl, and 50.0 μL of 187.0 μM $KMnO_4$ were added to the cell. After electrodepositing Ag for 200 s at -0.300 V, a quiet time at 0 V for 10 s, and stripping from E_i = 0 V to E_f = 0.220 V at υ = 10 mV/s, the charge under each peak was measured. In the second experiment, 50.0 μL of 75.0 pM citrate-capped AgNP, 125.0 μL of PBCl, and 50.0 μL of 187.0 μM $KMnO_4$ were added to the cell. At this point, the same electrochemical procedure as in the first experiment was performed. Charges of 187 ± 18 and 200 ± 29 nC were recorded for the first and second experiments, respectively (Figure S4a). Although the position ($Ag^+ + e = Ag$, E° = 0.7991 V vs NHE; $AgCl + e = Ag^+ + Cl^-$, E°= 0.2223 V vs NHE)[1] and shape of the stripping peak vary between the two types of experiment, the charges measured are not statistically different. In addition, the charges measured with different experimental setups (*Facing Up* vs *Facing Down*, Figure S1a and S1b, respectively) showed no statistical difference between the charges recovered (*Facing Up* = 214 ± 9 nC, *Facing Down* = 211 ± 7 nC). These values would be much different from each other if AgCl precipitated from solution. Therefore, we conclude that the presence of NaCl at high concentration does not affect the electrochemical detection method discussed in the main text.

In addition to Cl-, we also studied the effect of PO_4^{3-} on the electrochemistry. In this case, the experiment was carried out using the conventional electrochemical setup in the *Facing*

down configuration (Figure S1b). First, 30.0 μL of 750.0 pM citrate-capped AgNP, 125.0 μL of aqueous 0.1 M phosphate buffer (pH 7.4) or 0.1 M KNO_3, and 50.0 μL of 187.0 μM $KMnO_4$ were added to the cell. Second, after electrodepositing Ag for 200 s at -0.300 V, a quiet time at 0 V for 10 s, and stripping from E_i = 0 V to E_f = 0.220 V at υ = 10 mV/s, the charge under each peak was measured. Figure S4b shows that the charges measured using either PO_4^{3-} or NO_3^- ($AgNO_3$ is very soluble) are statistically the same.

As discussed in the main text, we attribute these results to the presence of $KMnO_4$ solubilizing Ag^+ in solution even in the presence of a high concentration Cl^- and PO_4^{3-}, which would otherwise precipitate Ag^+ as AgCl (K_{sp} = $1.8x10^{-10}$)[2] and Ag_3PO_4 (K_{sp} = $1.4x10^{-16}$)[2].

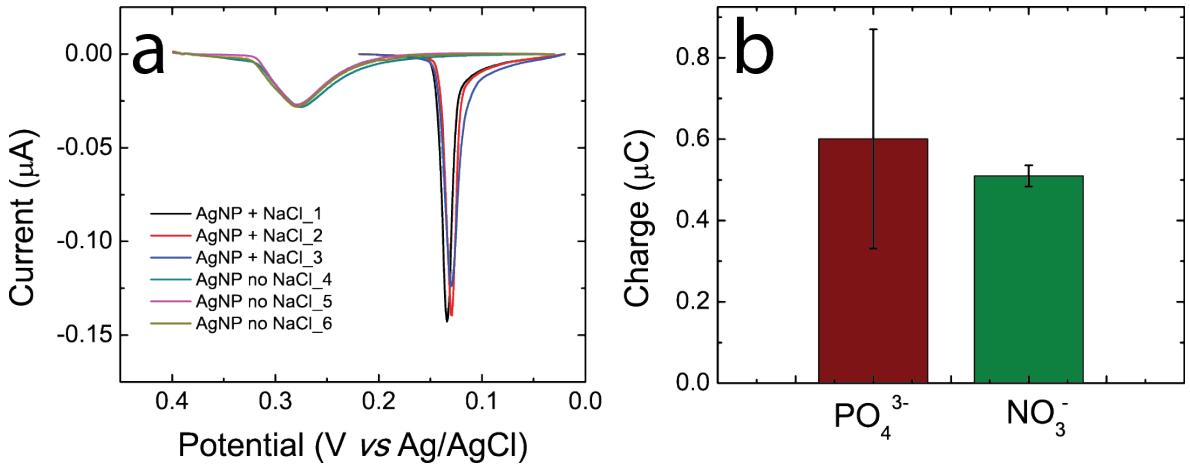

Figure S4. Ag^+ solubility in PBCl. (a) ASVs obtained in the conventional electrochemical cell in the presence and absence of 100.0 mM NaCl.(b) Histogram showing the electrochemical signal obtained with 0.1 M phosphate buffer (pH 7.4) and 0.1 M KNO_3. All experiments were performed in triplicate. See text for details.

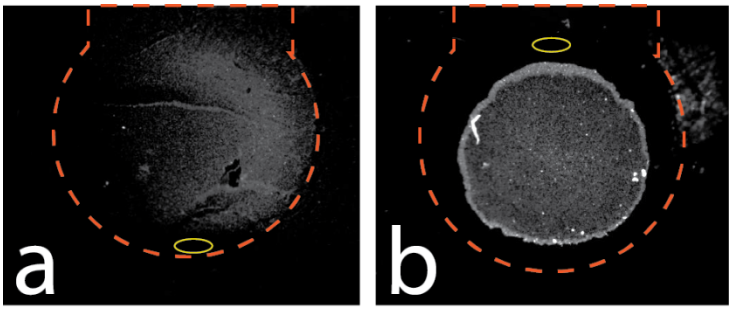

Figure S5. Micrographs showing the background fluorescence of the *o*Slip working electrode (WE) for the Test and (b) Control experiments represented in Figure 3 of the main text. The orange-dashed lines represent the location of the WE. The yellow lines show the areas used to measure the background fluorescence intensity. Note that equivalent areas were used and each experiment was performed in triplicate.

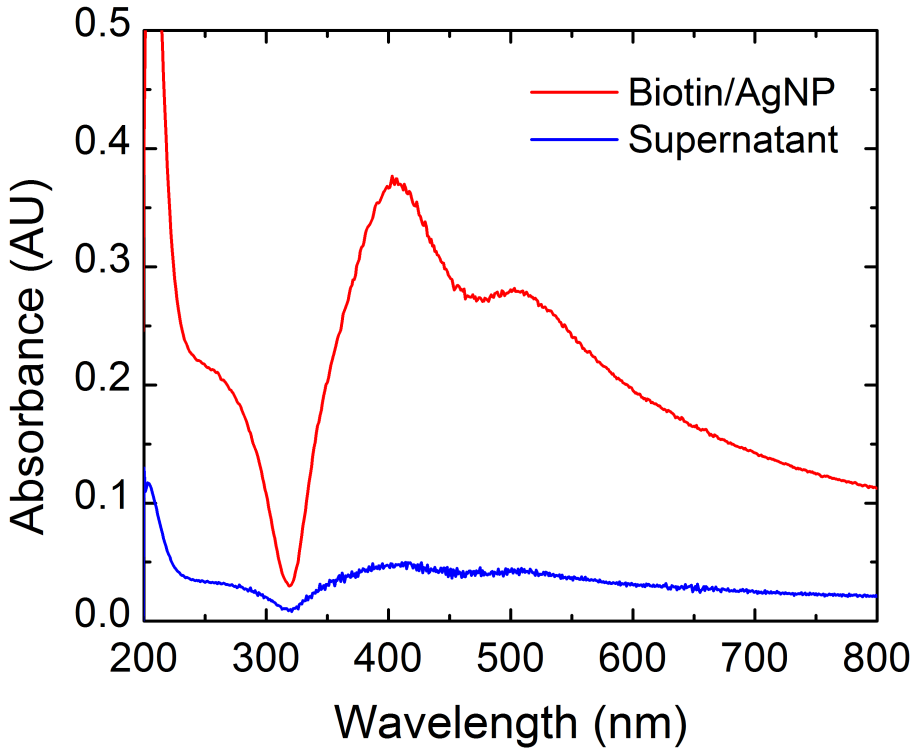

Figure S6. UV-Vis spectra showing the formation of the AgNP/biotin/streptavidin/magnetic microbead model analyte. The red trace corresponds to the biotinylated AgNP absorbance before incubation with streptavidin-coated magnetic microbeads. The blue trace corresponds to the supernatant absorbance after incubating biotinylated AgNPs with streptavidin-coated magnetic microbeads.

Optimization of the electrochemical signal using the conventional electrochemical setup

The maximum charge obtained using the conventional electrochemical cell was optimized by changing the number of moles of $KMnO_4$ added, while keeping the number of AgNPs constant. The experiment was carried out by dispensing 125.0 μL of PBCl and 50.0 μL of 75.0 pM citrate-capped AgNPs into the PTFE cell in the *Facing Up* configuration (Figure S1a). Next, 50.0 μL of different concentrations of $KMnO_4$ were added and mixed thoroughly. The electrodeposition and dissolution steps were carried out as described in the "Electrochemical characterization of AgNP detection using a conventional electrochemical cell" section of the main text.

Figure S7 shows the results of this experiment, which resemble those obtained in the *o*Slip optimization experiment shown in Figure 2 of the main text. Here, however, a maximum in the plot is obtained at 9.56 nmol of $KMnO_4$.

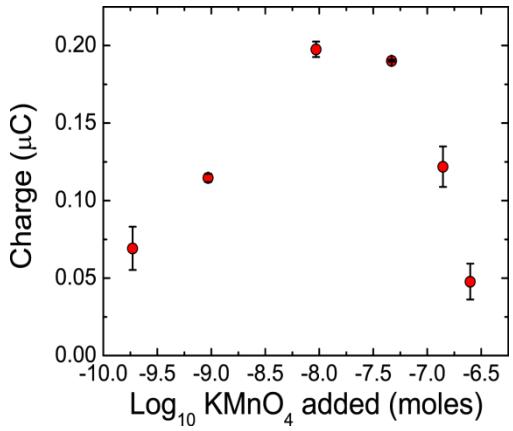

Figure S7. Optimization of the electrochemical signal in the conventional electrochemical cell. Plot of charge under the ASV peak as a function of the number of $KMnO_4$ moles added. The number of Ag moles was kept constant. The error bars for each data point represent the standard deviation of three different measurements.

Insulation of the electrode surface by MnO_2

At neutral pH, $KMnO_4$ is reduced to MnO_2 according to the following equation:[3]

$$MnO_4^- + 2H_2O + 3e \leftrightarrow MnO_2 + 4OH^-$$

Therefore, the higher the $KMnO_4$ concentration used, the higher the concentration of MnO_2 produced and the more the electrode becomes electronically insulated. Figure S8 shows micrographs of a GCE before and after electrodeposition and stripping steps (in the absence of AgNPs) at $KMnO_4$ concentrations of 5.0 mM (a and c) and 187.0 μM (b and d). The micrographs reveal a thicker layer of MnO_2 when a higher concentration of $KMnO_4$ is used. Additional evidence for the presence of MnO_2 is demonstrated by the more resistive ASV wave when the concentration of $KMnO_4$ = 5.0 mM (Figure S8e). Figure S1c demonstrates this effect is consistent in both the *Facing Up* and *Facing Down* cell configurations as the charges measured are the same (*Facing Up* = 214 ± 9 nC, *Facing Down* 211 ± 7 nC).

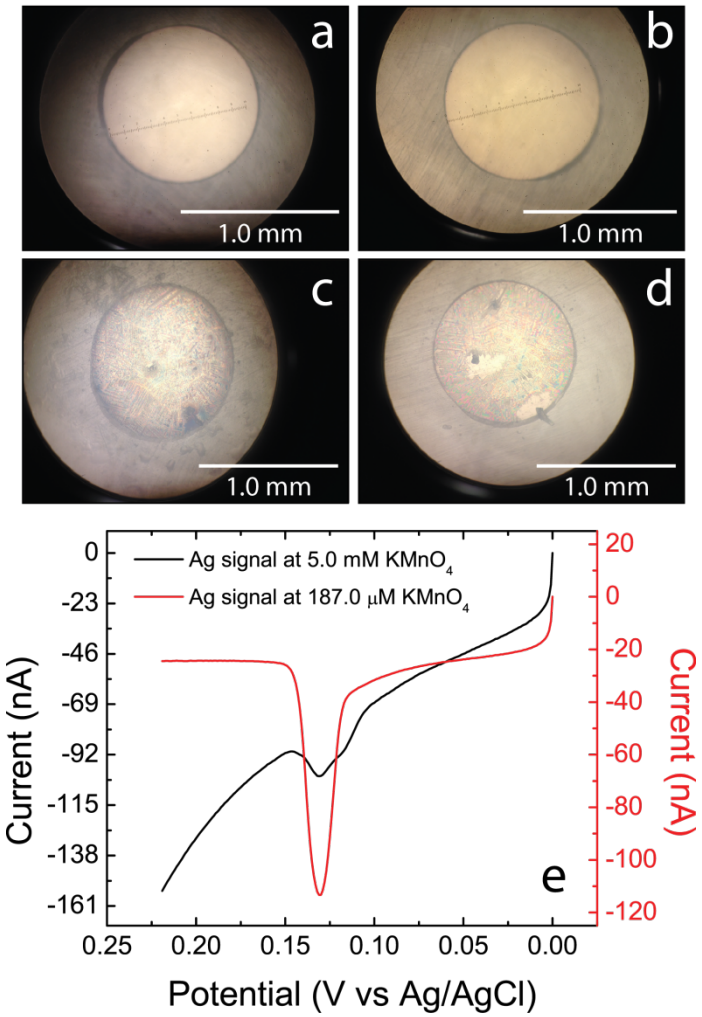

Figure S8. Effect of MnO_2 on the electrochemical signal using initial $KMnO_4$ concentrations of 5.0 mM and 187.0 μM. (a) GCE surface before the experiment at 5.0 mM $KMnO_4$. (b) GCE surface before the experiment at 187.0 μM $KMnO_4$. (c) GCE surface after the experiment at 5.0 mM $KMnO_4$. (d) GCE surface after the experiment at 187.0 μM $KMnO_4$. (e) Anodic stripping voltammograms in the presence of 5.0 mM (black trace) and 187.0 μM (red trace) $KMnO_4$.

Optimization of $KMnO_4$ re-solvation time in the *o*Slip

The waiting time between slipping Layer 3 into position 2 and the initiation of the electrodeposition step was optimized in order to maximize the amount of $KMnO_4$ that reaches the electrode surface to oxidize the AgNPs. This experiment was carried out by drying 4.0 μL of an aqueous solution containing 934.0 μM $KMnO_4$ onto the square reservoir on Layer 3 (see Scheme 1, main text), assembling the *o*Slip, and adding 50.0 μL of PBCl to the *Inlet*. Once the *Outlet* turned blue, Layer 3 was slipped into position 2. After different waiting times (5, 12, 30, and 120 s), cyclic voltammograms were recorded (from E_i = 0.600 V to E_f = -1.000 V vs cpQRE at υ = 100 mV/s).

Figure S9 shows a plot of the cathodic peak current as a function of the waiting time. The ohmic drop for every *o*Slip was compensated before each measurement. This compensation takes approximately 10 s; therefore, the 5 s data point was obtained by fixing the potentiostat to compensate for an ohmic drop of 4.0 kΩ. On the basis of these results, 12 s was chosen as the ideal waiting time for all *o*Slip experiments. The inset of Figure S9 shows cyclic voltammograms for three different *o*Slips for the reduction of $KMnO_4$ after a waiting time of 12 s.

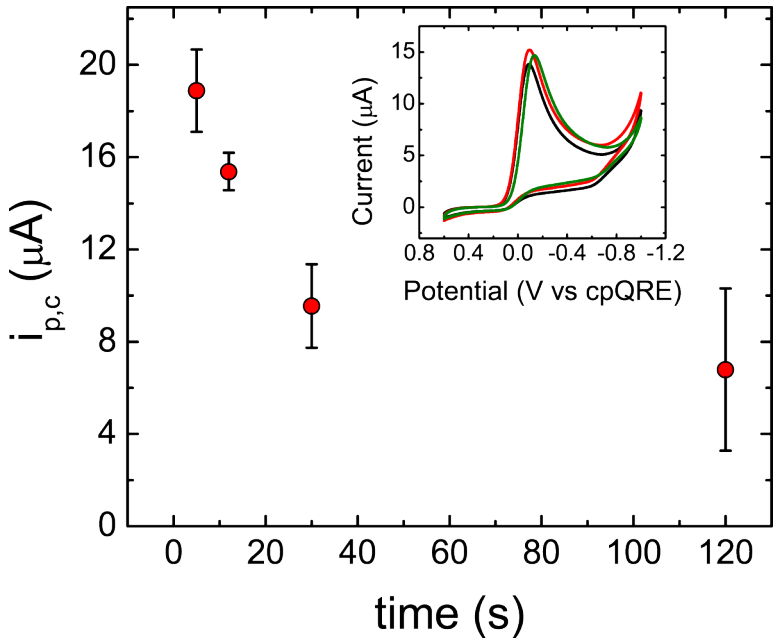

Figure S9. Time-dependent study of $KMnO_4$ re-solvation in the *o*Slip. The error bars on each data point represent the standard deviation obtained for three different *o*Slips. Inset: cyclic voltammograms of $KMnO_4$ obtained using three independently fabricated *o*Slips. The voltammograms were initiated 12 s after slipping Layer 3 into position 2 (Scheme 1c, main text).

References

1. Bard, A., J.; Faulkner, L. R. *Electrochemical Methods. Funtamentals and Applications*; 2nd Edition.; John Wiley & Sons: New York, 2001.
2. Dean, J. A. *Lange's Handbook of Chemistry*; 13th ed.; McGraw-Hill: New York, 1985.
3. Burgot, J.-L. Oxidations with Permanganate, Dichromate, and Ceric Ions Some Titration Methods Involving a Reduction Reaction. In *Ionic Equilibria in Analytical Chemistry*; Springer: New York, 2010.